Video Article

Non-invasive Optical Measurement of Cerebral Metabolism and Hemodynamics in Infants

Pei-Yi Lin[1], Nadege Roche-Labarbe[1,2], Mathieu Dehaes[3], Stefan Carp[1], Angela Fenoglio[3], Beniamino Barbieri[4], Katherine Hagan[1], P. Ellen Grant[3], Maria Angela Franceschini[1]

[1]Athinoula A. Martinos Center for Biomedical Imaging, Massachusetts General Hospital, Harvard Medical School

[2]Lab. PALM, Université de Caen Basse-Normandie

[3]Fetal-Neonatal Neuroimaging and Developmental Science Center, Boston Children's Hospital, Harvard Medical School

[4]ISS, INC.

Correspondence to: Pei-Yi Lin at ivylin@nmr.mgh.harvard.edu

URL: http://www.jove.com/video/4379
DOI: doi:10.3791/4379

Keywords: Medicine, Issue 73, Developmental Biology, Neurobiology, Neuroscience, Biomedical Engineering, Anatomy, Physiology, Near infrared spectroscopy, diffuse correlation spectroscopy, cerebral hemodynamic, cerebral metabolism, brain injury screening, brain health, brain development, newborns, neonates, imaging, clinical techniques

Date Published: 3/14/2013

Citation: Lin, P.Y., Roche-Labarbe, N., Dehaes, M., Carp, S., Fenoglio, A., Barbieri, B., Hagan, K., Grant, P.E., Franceschini, M.A. Non-invasive Optical Measurement of Cerebral Metabolism and Hemodynamics in Infants. *J. Vis. Exp.* (73), e4379, doi:10.3791/4379 (2013).

Abstract

Perinatal brain injury remains a significant cause of infant mortality and morbidity, but there is not yet an effective bedside tool that can accurately screen for brain injury, monitor injury evolution, or assess response to therapy. The energy used by neurons is derived largely from tissue oxidative metabolism, and neural hyperactivity and cell death are reflected by corresponding changes in cerebral oxygen metabolism ($CMRO_2$). Thus, measures of $CMRO_2$ are reflective of neuronal viability and provide critical diagnostic information, making $CMRO_2$ an ideal target for bedside measurement of brain health.

Brain-imaging techniques such as positron emission tomography (PET) and single-photon emission computed tomography (SPECT) yield measures of cerebral glucose and oxygen metabolism, but these techniques require the administration of radionucleotides, so they are used in only the most acute cases.

Continuous-wave near-infrared spectroscopy (CWNIRS) provides non-invasive and non-ionizing radiation measures of hemoglobin oxygen saturation (SO_2) as a surrogate for cerebral oxygen consumption. However, SO_2 is less than ideal as a surrogate for cerebral oxygen metabolism as it is influenced by both oxygen delivery and consumption. Furthermore, measurements of SO_2 are not sensitive enough to detect brain injury hours after the insult [1,2], because oxygen consumption and delivery reach equilibrium after acute transients [3]. We investigated the possibility of using more sophisticated NIRS optical methods to quantify cerebral oxygen metabolism at the bedside in healthy and brain-injured newborns. More specifically, we combined the frequency-domain NIRS (FDNIRS) measure of SO_2 with the diffuse correlation spectroscopy (DCS) measure of blood flow index (CBF_i) to yield an index of $CMRO_2$ ($CMRO_{2i}$) [4,5].

With the combined FDNIRS/DCS system we are able to quantify cerebral metabolism and hemodynamics. This represents an improvement over CWNIRS for detecting brain health, brain development, and response to therapy in neonates. Moreover, this method adheres to all neonatal intensive care unit (NICU) policies on infection control and institutional policies on laser safety. Future work will seek to integrate the two instruments to reduce acquisition time at the bedside and to implement real-time feedback on data quality to reduce the rate of data rejection.

Video Link

The video component of this article can be found at http://www.jove.com/video/4379/

Introduction

The FDNIRS device is a customized frequency-domain system from ISS Inc. with two identical sets of 8 laser diodes emitting at eight wavelengths ranging from 660 to 830 nm, and two photomultiplier tube (PMT) detectors. Sources and detectors are modulated at 110 MHz and 110 MHz plus 5 kHz, respectively, to achieve heterodyne detection [6]. Each laser diode is turned on for 10 msec in sequence, for a 160 msec total acquisition time per cycle. Sources and detectors are coupled to fiber optics and arranged in a row in an optical probe. The arrangement of fibers on the probe is such that it produces four different source-detector separations. By measuring transmitted light (amplitude attenuation and phase shift) at multiple distances, we can quantify the absorption (μa) and scattering (μs') coefficients of the tissue under observation. From the absorption coefficients at multiple wavelengths, we then estimate the absolute values of oxygenated (HbO) and deoxygenated (HbR) hemoglobin concentrations [7], cerebral blood volume (CBV) and hemoglobin oxygen saturation (SO_2).

The DCS device is a home-built system similar to the one developed by Drs. Arjun Yodh and Turgut Durduran at the University of Pennsylvania [8,9]. The DCS system that consists of a solid-state, long coherence laser at 785 nm, four photon-counting avalanche photodiode (APD) detectors

(EG&G Perkin Elmer SPCM-AQRH) featuring low dark counts (<50 counts/sec) and a high quantum yield (>40% at 785 nm), and a four channel, 256-bin multi-tau correlator, with 200 nsec resolution. With the DCS we measure microvascular blood flow in cerebral cortex by quantifying the temporal intensity fluctuations of multiply scattered light that arises from Doppler shifts produced by moving red blood cells. The technique, similar to laser Doppler blood flowmetry (*i.e.* they are Fourier Transform analogs), measures an autocorrelation function of the intensity fluctuations of each detector channel computed by a digital correlator over a delay time range of 200 nsec - 0.5 sec. The correlator computes the temporal intensity auto-correlation of the light re-emerging from tissue. We then fit the diffusion correlation equation to the measured autocorrelation function, acquired sequentially, about once per second, to obtain the blood flow index (CBF_i) [10,11]. DCS measures of blood flow changes have been extensively validated [12,13]. By combining the FDNIRS measures of SO_2 with the DCS measures of CBF_i, we achieve an estimate of cerebral oxygen metabolism ($CMRO_{2i}$).

Protocol

1. Preparation for Bedside Measures

1. The FDNIRS and the DCS systems are compact and easy to move on a small cart to the infant's bedside in the hospital (**Figure 1**).
2. After moving the cart with the devices to the bedside, turn on the systems and connect the optical probe to the FDNIRS and DCS devices. Ensure that two experimenters are present for every measurement: one to manage the instruments and computer, and one to hold the probe.
3. Choose the appropriate probe according to the infant's postmenstrual age (PMA). The optical probe with FDNIRS source-detector separations of 1, 1.5, 2 and 2.5 cm is used for infants <37 wks PMA and the probe with FDNIRS separations 1.5, 2, 2.5 and 3 cm is used for older infants **(Figure 2-A)**. The choice of shorter source-detector separations is dictated by preterm infants' small size and larger head curvature. When using a larger probe with a preterm infant, the relatively smaller size of the baby's head and its significant curvature together impede effective contact between the infant's head and all sources and detectors. For this reason, the probe with FDNIRS source-detector separations of 1, 1.5, 2 and 2.5 cm is fitting for use with preterm infants. Our research has verified that the chosen source-detector separations are sufficient to measure optical properties of the cerebral cortex of both preterm and term [14]. DCS source and detector fibers are arranged in a row parallel to the FDNIRS fibers with source-detector distances of 1.5 (one detector) and 2 cm (three detectors) in both premature and term infants probes.
4. Sanitize the optical probes with a Sani-cloth disinfecting wipe and insert the probe and fibers into a single-use polypropylene plastic sleeve.

2. FDNIRS Gain Settings and Calibration

1. Open the FDNIRS Graphical User Interface (GUI) and select the program settings file corresponding to the probe and calibration block being used.
2. To adjust detector gains, gently place the probe on an area of the subject's head without hair (preferably the left side of the forehead) and maintain it in the same position without applying any pressure. Turn on sources and detectors and adjust PMT voltage until the amplitude of any of the source lasers reaches 20,000 counts. 32,000 counts is the maximum digitization of the analog to digital acquisition card, and gains need to be set below that threshold to avoid saturation during data acquisition. The gains should be set in the frontal area because this region generally has the lowest absorption of laser light and is therefore most prone to saturation.
3. Turn off the sources and detectors and return the probe to the calibration block. The lasers need to be turned off when moving the probe for eye safety; the detectors need to be turned off because PMTs are very sensitive and exposure to any bright light increases background noise and may permanently damage them.
4. With the probe back on the calibration block, use the neutral density (ND) filter if any source-detector pair saturates. Different ND filters may be selected due to optimizing gains in infants with different skin tones Hold the probe still for 16 sec while running the calibration procedure. Since we do not physically move one source to different distances from a single detector to achieve a multi-distance scheme, but instead use four combinations of two independent sources and two independent detectors, we need to calibrate for the different power of the two sources and the different gains of the two detectors. By measuring a calibration block of known optical properties, we estimate the amplitude and phase correction factors needed to recover the absorption and scattering coefficients of the calibration block.
5. After calibration, acquire 16 more sec of data on the block and visually assess the adequacy of the calibration with an in-house MATLAB GUI. The measured μa and μs' should match the actual coefficients of the calibration block at all wavelengths. Recalibrate if the fit is poor.
6. If detector gains need to be changed, or source and detector fibers need to be disconnected during measurements, repeat the calibration procedure of the FDNIRS device.
7. At the end of the measurement session, acquire another 16 sec of data on the calibration block to verify whether the calibration was maintained during measurements on the subject. If the calibration has not been maintained, take a second calibration at the end of the measurement and apply to the acquired data.

3. DCS Settings

1. Open the in-house DCS data acquisition GUI and load the settings file corresponding to the optical probe being used.
2. Before starting measurements, verify that the laser power of the DCS source is appropriate for skin exposure by measuring the laser power of the DCS source with a power meter and checking the spot size with an IR viewing card (the laser emits at 785 nm, which is not visible). The DCS laser power is ~60 mW and coupled to a relatively small diameter fiber (400-600 μm). To meet ANSI standards for skin exposure, the light at the probe must be attenuated and diffused across a large area. This is achieved by covering the tip of the fiber with a 3 mm diameter white Teflon sheet (**Figure 2-A**). The Teflon is highly scattering and widely diffuses the laser beam. At the bedside, ensure that the laser power at the probe is less than 25 mW and the spot size is larger than 3 mm in diameter. As for the FDNIRS, always turn off sources and detectors when moving the optical probe.
3. DCS detection is photon-counting and there is no APD gain adjustment as is required for the FDNIRS device. A flag in the acquisition software indicates if too much light is detected, in which case light coupling to either source or detector fibers needs to be reduced by turning

the fiber connectors. Adequate light detection is on the range of 200,000-4,000,000 detected photons (corresponding to -26~0 dB on the computer display). Avoid excessive room light to reduce background noise.
4. The DCS does not require calibration to measure CBF_i. Blood flow is proportional to the time it takes to lose correlation. A solid block does not suffice to check signal quality because there are no moving scattering particles to cause decay. An experimenter's arm instead shows decay -- the faster the blood flow, the steeper the decay.

4. Data Acquisition

1. While FDNIRS and DCS measurements can be done quickly in sequence, first measure all locations with one device and then repeat the same progression with the other device, using independent acquisition software corresponding to each.
2. Measure seven locations covering frontal, temporal and parietal areas, according to a 10-20 system (Fp1, FpZ, FP2, C3, C4, P3, P4), in sequence (**Figure 2-B**). Part the hair along the source-detector line and place the probe on that area of the head.
3. Turn on FDNIRS lasers and detectors and check the signal quality: amplitude counts should be between 2,000 and 20,000 and phase shifts SNR <2 degrees. If outside of these ranges, reposition the probe, ensuring hair is parted and all sources and detectors are in contact with the skin.
4. Acquire data for 16 sec. Repeat measurements up to three times in each location (**Figure 2-C**), parting the hair and repositioning the probe in a slightly different spot for each acquisition. This is done to minimize effect of local inhomogeneities such as hair and superficial large vessels and to provide values representative of a region, rather than a single spot.
5. Turn on the DCS laser and detectors and acquire data for 10 sec. Reposition the probe and repeat the acquisitions (as with the FDNIRS measures).
6. Turn off all lasers when moving the probe between locations. Data collection in all seven locations is not always possible. Discontinue measurements if the subject manifests any sign of distress or motion. Retry the acquisition if possible. EEG electrodes or respiratory equipment may also preclude measurements in some locations.

5. Measure of Systemic Parameters

1. For the calculation of $CMRO_{2i}$, two systemic parameters, arterial oxygenation (SaO_2) and hemoglobin in the blood (HGB), must be acquired. HGB is also needed to calculate CBV. While conventional pulse oximetry provides measures of SaO_2, HGB is conventionally measured with a blood test. A new pulse oximeter, developed by Masimo Corporation, is able to measure HGB non-invasively by using multiple wavelengths. The device is FDA-approved for infants >3 kg, and allows for a quick bedside measure of both SaO_2 and HGB.
2. Record SaO_2 and HGB using a Masimo pulse oximeter (Pronto spot check pulse co-oximeter). For these measurements, attach an adhesive single-use sensor to the big toe of the baby's foot. HGB will be displayed on the monitor within a few seconds.
3. When it is not possible to use the Masimo pulse co-oximeter, measure SaO_2 with other FDA-approved pulse oximeters. HGB can be either recovered from patients' clinical charts or estimated using normative values.

6. Data Analysis

1. Open an in-house post-processing data analysis GUI using MATLAB. This software not only estimates all hemodynamic parameters, but also uses the redundancy of data to automatically assess measurement quality and constrain results.
2. Automatic objective criteria for quality control consist of discarding data for FDNIRS if: R2 < 0.98 for the model fit of the experimental data, p-value > 0.02 for the Pearson product moment correlation coefficient between the eight measured absorption coefficients and the hemoglobin fit (**Figure 3-A**), p-value > 0.02 for the linear fit of the reduced scattering coefficients versus wavelength (**Figure 3-B**) [15]. If more than 33 percent of the data merits discarding, the whole set is discarded. For the DCS, data is discarded if: the tail of the fitting curve differs from 1 by more than 0.02, the cumulative variation among the 3 first points of the curve is more than 0.1, or the average value of the 3 first points is more than 1.6 (**Figure 4**). If more than 50 percent of curves are discarded, or the fit values have a coefficient of variation > 15 percent, the whole set is discarded[15].
3. Calculate absolute HbO and HbR concentrations by fitting the absorption coefficients at all wavelengths, using literature values for Hb extinction coefficients [16] and a 75 percent concentration of water in tissue [17]. Derive total hemoglobin concentration (HbT = HbO + HbR) and SO_2 (HbO / HbT) from HbO and HbR concentrations.
4. Estimate cerebral blood volume using the equation described in Ijichi *et al* [18]. CBV= (HbT × MW_{Hb}) / (HGB × D_{bt}), where MW_{Hb} = 64,500 [g/Mol] is the molecular weight of Hb, and D_{bt} = 1.05 g/ml is the brain tissue density.
5. Calculate CBF_i by fitting the measured temporal autocorrelation functions to the diffusion correlation equation. The detailed theoretical framework to calculate CBF_i is in Boas *et al.* and Boas and Yodh [10,11]. In the equations, use individual absorption coefficients measured from FDNIRS and an average of the scattering coefficients across the whole population.
6. Calculate the index of cerebral oxygen consumption by using the FDNIRS measure of SO_2 and the DCS measure of CBFi with the following equation: $CMRO_{2i}$ = (HGB × CBFi × (SaO_2 - SO_2)) / (4 × MW_{Hb} × β)[15], where the factor 4 reflects the four O_2 molecules bound to each hemoglobin and β is the percent contribution of the venous compartment to the hemoglobin oxygenation measurement [19].

Representative Results

In the past five years we have demonstrated the feasibility and clinical utility of the proposed method. In particular, we have shown $CMRO_2$ to be more representative of brain health and development than SO_2.

In a cross-sectional study on more than 50 healthy infants, we found that while CBV is more than double during the first year of life, SO_2 remains constant [4] (**Figure 5**). In a study on 70 healthy newborns we also found that SO_2 is constant across brain regions while $CMRO_{2i}$, CBV and CBF are higher in temporal and parietal regions than in the frontal region (**Figure 6**)[20], which is consistent with PET glucose uptake findings [21]. In both

of our studies, the constant SO_2, within a 60-70 percent range indicates that oxygen delivery closely matches local consumption, while CBV, CBF and $CMRO_2$ are more tightly coupled with neural development.

To verify that $CMRO_{2i}$ is a better screening tool than SO_2 in detecting neonatal brain injury, we measured brain injured infants during the acute phase [5], and (in a few infants) during the chronic phase several months after injury. Results in **Figure 7** show how SO_2 is not significantly altered by brain injury in both early (1-15 days after insult) and chronic (months after injury) stages, while $CMRO_{2i}$ is significantly different than normal during both the acute and chronic stages. Specifically, $CMRO_{2i}$ is elevated during the acute phase because of seizure activity after brain injury, and lower than normal during the chronic phase due to neuronal loss.

Infants with hypoxic ischemic injuries are currently treated with therapeutic hypothermia (TH) to lower brain metabolism and reduce damage after the hypoxic insult. Therapeutic hypothermia is maintained for three days and we have been able to monitor 11 infants during treatment (**Figure 8**). We found that $CMRO_{2i}$ significantly decreases to levels below normal during TH, and this decrease seems to be related to response to therapy and developmental outcome. These preliminary results suggest that the FDNIRS-DCS method may be able to guide and optimize hypothermia therapy.

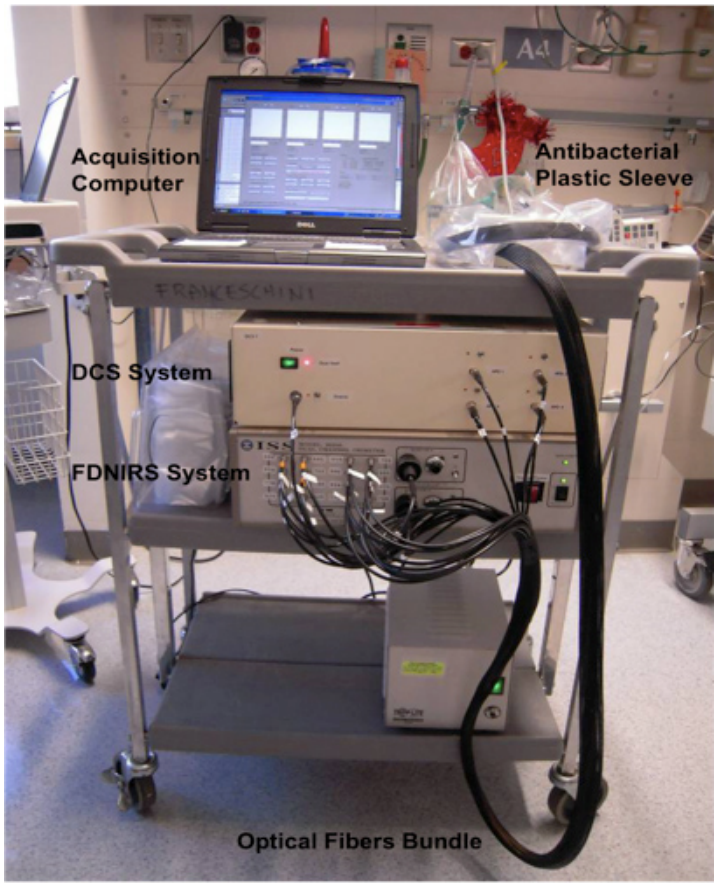

Figure 1. Picture of the cart with the FDNIRS and DCS devices. The two instruments are compact enough to fit on a small cart that can be moved to the infant's bedside in the NICU.

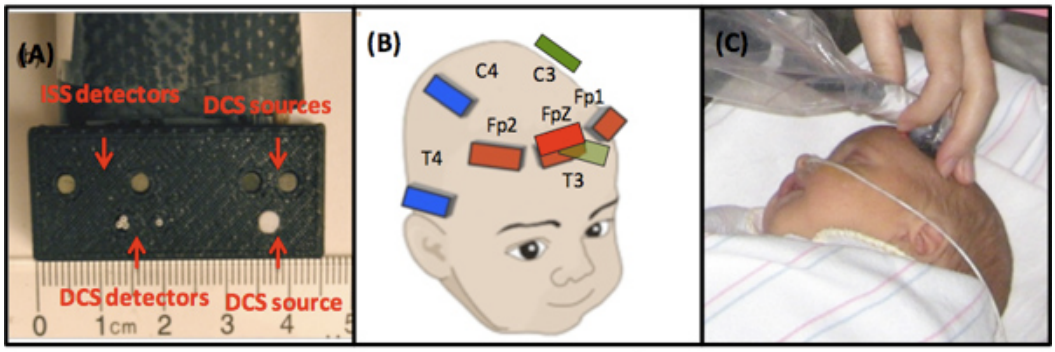

Figure 2. (A) Optical probe configuration. **(B)** The measurement location scheme. **(C)** A photo of a typical FDNIRS-DCS measurement on an infant.

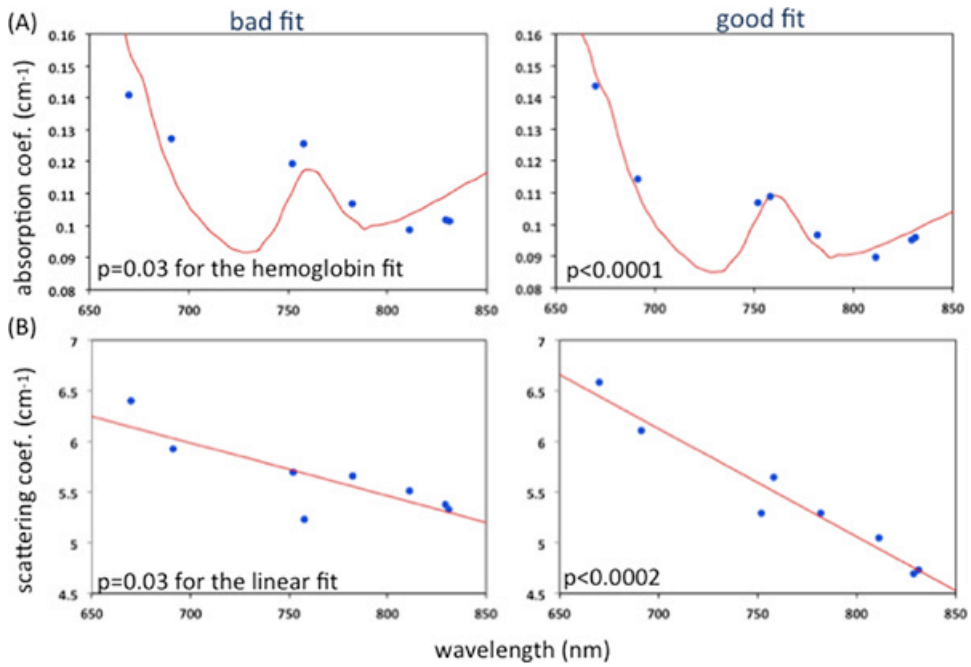

Figure 3. Representative examples of good and bad fit of measured **(A)** absorption coefficients and the hemoglobin fit **(B)** scattering coefficients and the linear fit. P-value > 0.02 refers to a bad fit. Click here to view larger figure.

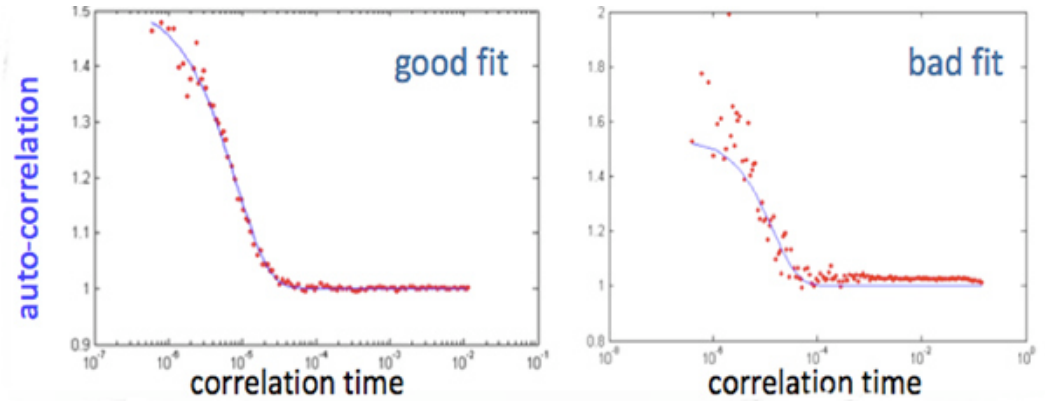

Figure 4. A representative example of good and bad fit of an autocorrelation function of the intensity fluctuations computed by a correlator over a delay time range of 200 nsec - 0.5 sec. In the bad fit figure the tail of the fitting curve differs from 1 by more than 0.02 and the variation of the 3 first points is more than 0.1. Click here to view larger figure.

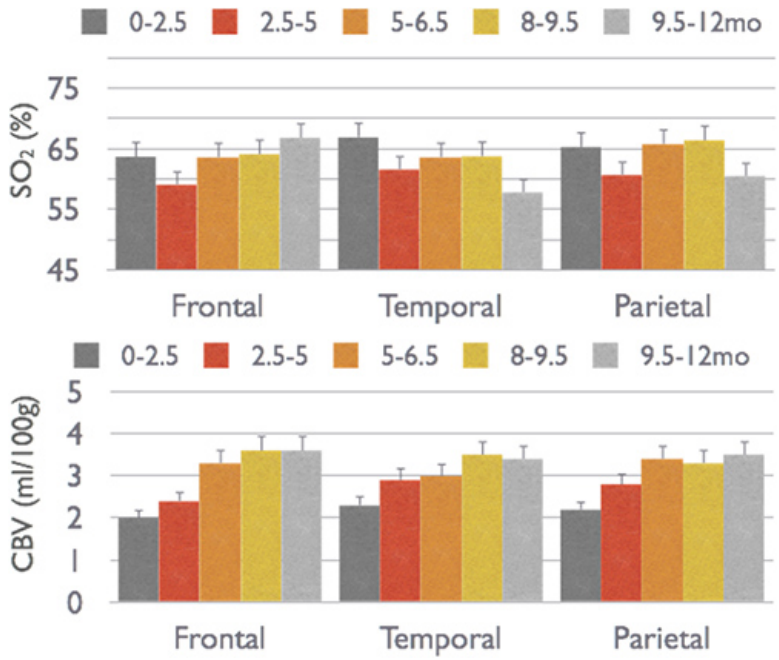

Figure 5. Changes in CBV and SO_2 across frontal, temporal and parietal cortical regions in infants from birth to one year of age.

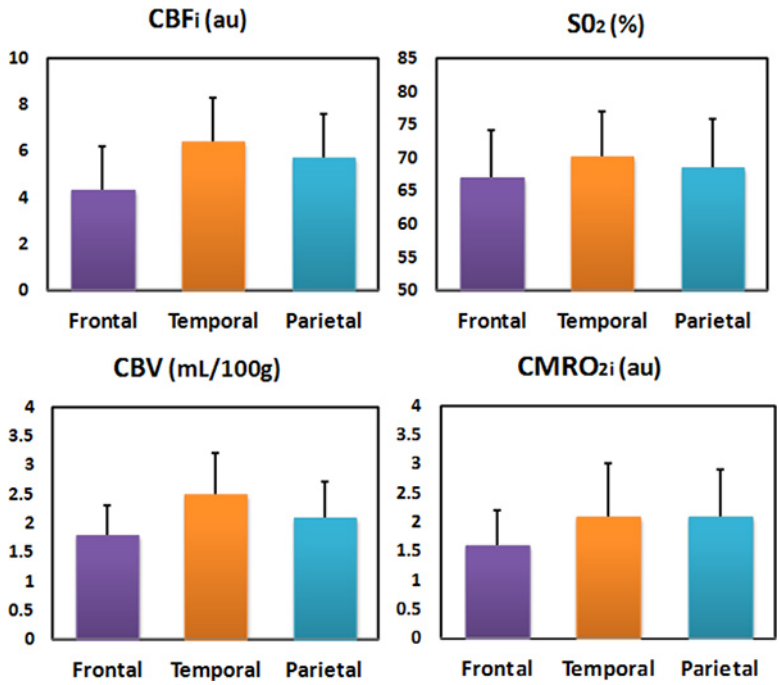

Figure 6. CBF, SO_2, CBV and $CMRO_{2i}$ of the frontal, temporal and parietal regions in 70 healthy newborns.

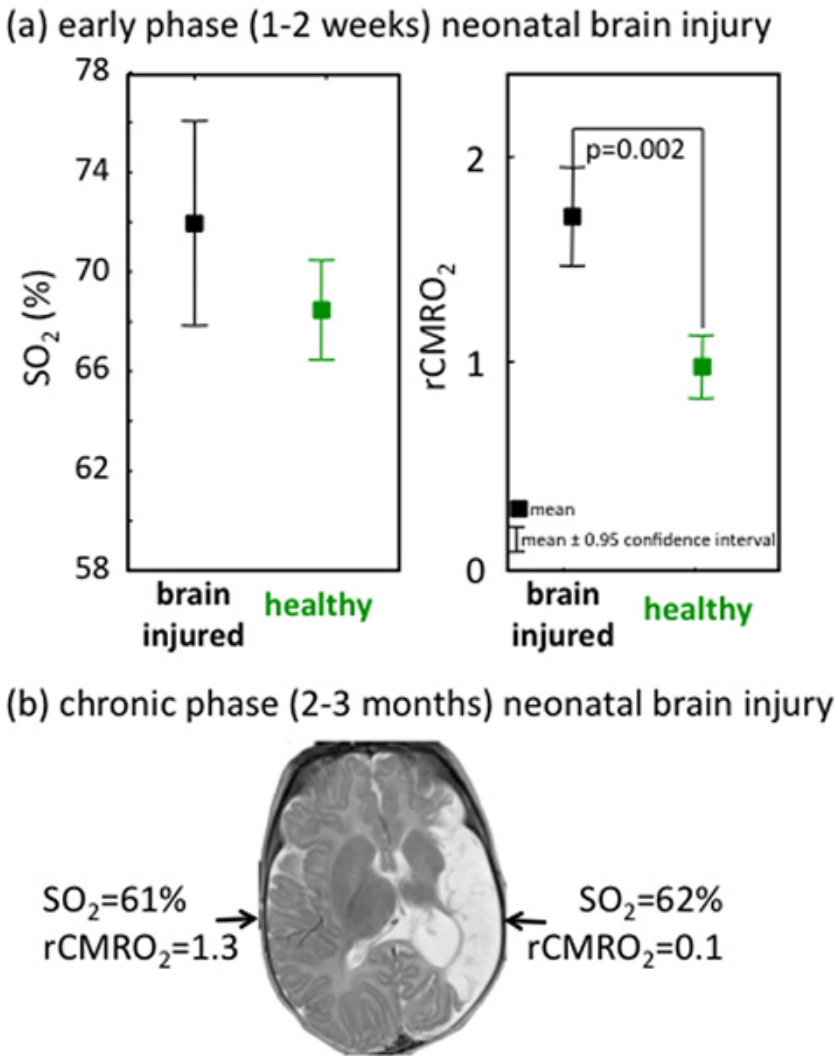

Figure 7. Examples of abnormal oxygen consumption and normal SO_2 after brain injury in infants. Brain injury is marked by changes in $CMRO_2$ with respect to normal while SO_2 is not significantly different from normal. Please note that in these two figures, $CMRO_2$ was calculated using the Grubb relationship, because the DCS measure was not available at the time of those measurements.

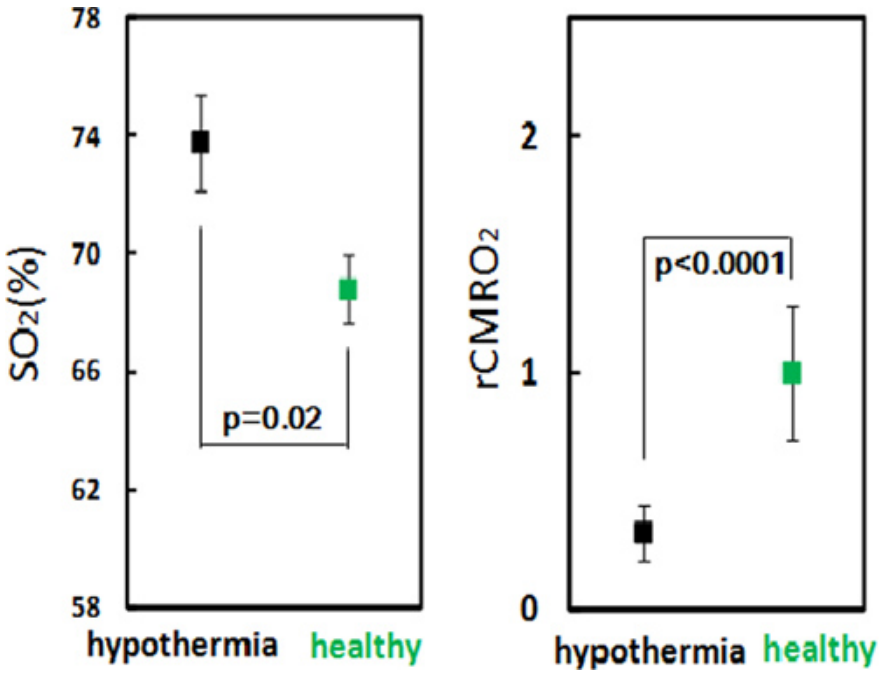

Figure 8. $rCMRO_2$ of 11 infants during therapeutic hypothermia vs. age-matched healthy controls. Oxygen metabolism is strongly reduced in all infants with hypothermia therapy.

Discussion

We demonstrated a quantitative measurement of cerebral hemodynamic and metabolism with FDNIRS and DCS in the neonatal population. The probe configuration is optimized for measuring neonatal cerebral cortex [14]. Blood flow changes measured by DCS have been extensively validated against other techniques in animal and human studies [22,23]. By using a direct DCS measure of blood flow, we are able to reduce the variance in the calculation of $CMRO_{2i}$ [24]. The variance from repeated measures was also smaller than the changes between brain regions and with age [20].

From our previous results, CBFi and $CMRO_{2i}$ showed significant changes with PMA in healthy preterm neonates. The measure of $CMRO_{2i}$ is better able to detect brain damage than the measure of SO_2. This suggests that combined measures of vascular and metabolic parameters serve as more robust biomarkers of neonatal brain health and development than oxygen saturation alone. Technical improvements will focus on the integration of two instruments to reduce acquisition time 35-40% per session and the implementation of real-time feedback on data quality to reduce the frequency of discarded measures. In the near future, this system can be delivered to clinical end-users as a novel bedside monitor of altered cerebral oxygen metabolism. By measuring trajectories of $CMRO_2$ over time may also increase clinical significance and predict outcomes. This tool could ultimately make a significant contribution towards improved management of neonatal brain injury.

Disclosures

Maria Angela Franceschini, her husband David Boas, and Beniamino Barbieri (ISS Inc) hold patents on this technology.

Acknowledgements

The authors thank all the families for their participation in this study and the nurses, physicians, and staff in the Neonatal ICU, the Special Care Nursery, Pediatric Neurology, and the maternity units at Massachusetts General Hospital, Brigham and Women's Hospital and Boston Children's Hospital for their help and support. In particular we thank Linda J. Van Marter, Robert M. Insoft, Jonathan H. Cronin, Julianne Mazzawi, and Steven A. Ringer. The authors also thank Marcia Kocienski-Filip, Yvonne Sheldon, Alpna Aggarwall, Maddy Artunguada and Genevieve Nave for their assistance during measurements. This project is supported by NIH R01-HD042908, R21- HD058725, P41- RR14075 and R43-HD071761. Marcia Kocienski-Filip and Yvonne Sheldon are supported by the Clinical Translational Science Award UL1RR025758 to Harvard University and Brigham and Women's Hospital from the National Center for Research Resources. The content is solely the responsibility of the authors and does not necessarily represent the official views of the National Center for Research Resources or the National Institutes of Health.

References

1. Zaramella, P., *et al.* Can tissue oxygenation index (TOI) and cotside neurophysiological variables predict outcome in depressed/asphyxiated newborn infants? *Early Hum. Dev.* **83**, 483-489 (2007).
2. van Bel, F., Lemmers, P., & Naulaers, G. Monitoring neonatal regional cerebral oxygen saturation in clinical practice: value and pitfalls. *Neonatology.* **94**, 237-244 (2008).

3. Boas, D.A. & Franceschini, M.A. Haemoglobin oxygen saturation as a biomarker: the problem and a solution. *Phil. Trans. R. Soc. A.* **369**, 4407-4424 (2011).
4. Franceschini, M.A., *et al.* Assessment of infant brain development with frequency-domain near-infrared spectroscopy. *Pediatr. Res.* **61**, 546-551 (2007).
5. Grant, P.E., *et al.* Increased cerebral blood volume and oxygen consumption in neonatal brain injury. *J. Cereb. Blood Flow Metab.* **29**, 1704-1713 (2009).
6. Feddersen, B.A., Piston, D.W., & Gratton, E. Digital parallel acquisition in frequency domain fluorimetry. *Rev. Sci. Instrum.* **60**, 2929-2936 (1989).
7. Fantini, S., *et al.* Frequency-domain multichannel optical detector for non-invasive tissue spectroscopy and oximetry. *Opt. Eng.* **34**, 34-42 (1995).
8. Cheung, C., Culver, J.P., Kasushi, T., Greenberg, J.H., & Yodh, A.G. *In vivo* cerebrovascular measurement combining diffuse near-infrared absorption and correlation spectroscopies. *Phys. Med. Biol.* **46**, 2053-2065 (2001).
9. Durduran, T., *et al.* Diffuse optical measurement of blood flow, blood oxygenation, and metabolism in a human brain during sensorimotor cortex activation. *Opt. Lett.* **29**, 1766-1768 (2004).
10. Boas, D.A., Campbell, L.E., & Yodh, A.G. Scattering and imaging with diffusing temporal field correlations. *Phys. Rev. Lett.* **75**, 1855-1859 (1995).
11. Boas, D.A. & Yodh, A.G. Spatially varying dynamical properties of turbid media probed with diffusing temporal light correlation. *J. Opt. Soc. Am. A.* **14**, 192-215 (1997).
12. Buckley, E.M., *et al.* Validation of diffuse correlation spectroscopic measurement of cerebral blood flow using phase-encoded velocity mapping magnetic resonance imaging. *J. Biomed. Opt.* **17**, 037007 (2012).
13. Irwin, D., *et al.* Influences of tissue absorption and scattering on diffuse correlation spectroscopy blood flow measurements. *Biomedical Optics Express.* **2**, 1969-1985 (2011).
14. Dehaes, M., *et al.* Assessment of the frequency-domain multi-distance method to evaluate the brain optical properties: Monte Carlo simulations from neonate to adult. *Biomed. Opt. Exp.* **2**, 552-567 (2011).
15. Roche-Labarbe, N., *et al.* Noninvasive optical measures of CBV, StO2, CBF index, and rCMRO2 in human premature neonates' brains in the first six weeks of life. *Hum. Brain Mapp.* **31**, 341-352 (2010).
16. Wray, S., Cope, M., Delpy, D.T., Wyatt, J.S., & Reynolds, E.O. Characterization of the near infrared absorption spectra of cytochrome aa3 and haemoglobin for the non-invasive monitoring of cerebral oxygenation. *Biochim. Biophys. Acta.* **933**, 184-192 (1988).
17. Wolthuis, R., *et al.* Determination of water concentration in brain tissue by Raman spectroscopy. *Anal. Chem.* **73**, 3915-3920 (2001).
18. Ijichi, S., *et al.* Developmental changes of optical properties in neonates determined by near-infrared time-resolved spectroscopy. *Pediatr. Res.* **58**, 568-573 (2005).
19. Watzman, H.M., *et al.* Arterial and venous contributions to near-infrared cerebral oximetry. *Anesthesiology.* **93**, 947 (2000).
20. Lin, P.Y., *et al.* Regional and hemispheric asymmetries of cerebral hemodynamic and oxygen metabolism in newborns. *Cereb. Cortex.*, doi:10.1093/cercor/bhs023 (2012).
21. Chugani, H.T. A critical period of brain development: studies of cerebral glucose utilization with PET. *Prev. Med.* **27**, 184-188 (1998).
22. Carp, S.A., Dai, G.P., Boas, D.A., Franceschini, M.A., & Kim, Y.R. Validation of diffuse correlation spectroscopy measurements of rodent cerebral blood flow with simultaneous arterial spin labeling MRI; towards MRI-optical continuous cerebral metabolic monitoring. *Biomed. Opt. Exp.* **1**, 553-565 (2010).
23. Durduran, T., *et al.* Optical measurement of cerebral hemodynamics and oxygen metabolism in neonates with congenital heart defects. *J. Biomed. Opt.* **15**, 037004 (2010).
24. Roche-Labarbe, N., *et al.* Near infrared spectroscopy assessment of cerebral oxygen metabolism in the developing premature brain. *J. Cereb. Blood Flow Metab.* **32**, 481-488 (2012).